Journal of Neurochemistry, 2007, **103**, 2651–2664 doi:10.1111/j.1471-4159.2007.04980.x

The α1 subunit of nicotinic acetylcholine receptors in the inner ear: transcriptional regulation by ATOH1 and co-expression with the γ subunit in hair cells

Deborah Scheffer,* Cyrille Sage,* Paola V. Plazas,† Mingqian Huang,‡ Carolina Wedemeyer,† Duan-Sun Zhang,§ Zheng-Yi Chen,‡ A. Belen Elgoyhen,† David P. Corey§ and Veronique Pingault*

**INSERM, Equipe Avenir, Unité 841, Creteil, France*
†Instituto de Investigaciones en Ingeniería Genética y Biología Molecular (CONICET) and Tercera Cátedra de Farmacología, Facultad de Medicina, Universidad de Buenos Aires, Argentina
‡Neurology Service, Massachusetts General Hospital, Boston, Massachusetts, USA
§Howard Hughes Medical Institute and Department of Neurobiology, Harvard Medical School, Boston, Massachusetts, USA

Abstract

Acetylcholine is a key neurotransmitter of the inner ear efferent system. In this study, we identify two novel nAChR subunits in the inner ear: α1 and γ, encoded by *Chrna1* and *Chrng*, respectively. *In situ* hybridization shows that the messages of these two subunits are present in vestibular and cochlear hair cells during early development. *Chrna1* and *Chrng* expression begin at embryonic stage E13.5 in the vestibular system and E17.5 in the organ of Corti. *Chrna1* message continues through P7, whereas *Chrng* is undetectable at post-natal stage P6. The α1 and γ subunits are known as muscle-type nAChR subunits and are surprisingly expressed in hair cells which are sensory-neural cells. We also show that ATOH1/MATH1, a transcription factor essential for hair cell development, directly activates *CHRNA1* transcription. Electrophoretic mobility-shift assays and supershift assays showed that ATOH1/E47 heterodimers selectively bind on two E boxes located in the proximal promoter of *CHRNA1*. Thus, *Chrna1* could be the first transcriptional target of ATOH1 in the inner ear. Co-expression in *Xenopus* oocytes of the α1 subunit does not change the electrophysiological properties of the α9α10 receptor. We suggest that hair cells transiently express α1γ-containing nAChRs in addition to α9α10, and that these may have a role during development of the inner ear innervation.

Keywords: ATOH1 protein, basic-helix-loop-helix transcription factors, cholinergic receptors, inner ear, hair cells.
J. Neurochem. (2007) **103**, 2651–2664.

The development of the mammalian inner ear begins with the formation of an otic placode through the thickening of the ectoderm adjacent to the developing hindbrain. Subsequently, the otic vesicle is produced through the invagination of the otic placode and undergoes a series of morphogenetic changes, to ultimately give rise to six sensory epithelia: the macula utriculi and sacculi and the three cristae ampularis in the vestibular system, and the organ of Corti in the cochlea (Riley and Phillips 2003; Barald and Kelley 2004). Each of these sensory epithelia is a mosaic of sensory hair cells separated by non-sensory supporting cells.

In the vestibular system, two types of hair cells, called type I and type II hair cells, differ in their response to vestibular stimuli and their post-synaptic connections (Eatock and Hurley 2003). In the organ of Corti, one row of inner hair cells (IHC) converts sounds into electrical signals and three rows of outer hair cells produce fast cochlear amplification (Fettiplace and Hackney 2006).

Atonal Homolog 1 (ATOH1, also called MATH1 for Mouse Atonal Homolog 1) is a major transcription factor involved in inner ear hair cell development. It is also involved in the cell fate of cerebellar granule neurons, D1 interneurons of the spinal cord, goblet, enteroendocrine and Paneth cells (Ben-Arie *et al.* 1997; Bermingham *et al.* 1999, 2001; Yang *et al.* 2001). Mice lacking ATOH1 do not develop hair cells (Bermingham *et al.* 1999), while its overexpression in the sensory or non-sensory epithelium of the cochlea is sufficient to induce a cell to adopt a hair-cell fate (Zheng and Gao 2000; Kawamoto *et al.* 2003; Woods *et al.* 2004). ATOH1 has been used with some success to reproduce hair cells in guinea pig and is considered as a possible tool for therapeutic intervention for deafness

Received May 21, 2007; revised manuscript received August 21, 2007; accepted August 23, 2007.

Address correspondence and reprint requests to Veronique Pingault, INSERM, U841, Departement de Genetique, Hopital Henri Mondor, Créteil, F-94010, France, E-mail: pingault@creteil.inserm.fr

Abbreviations used: ACh, acetylcholine; bHLH, basic helix-loop-helix; EMSA, electrophoretic mobility shift assay; GFP, green fluorescent protein; HEK, human embryonic kidney; IHC, inner hair cell; MRFs, myogenic regulatory factors; nAChR, nicotinic acetylcholine receptor; NE, nuclear extract; TET, tetracycline.

(Izumikawa *et al.* 2005). However, little is known about its molecular effects.

ATOH1 belongs to the tissue-specific class II of the basic-helix-loop-helix (bHLH) transcription factor family. bHLH transcription factors act synergistically to allow proper cell proliferation and/or cell fate determination of several cell types. They usually form dimers with a ubiquitously expressed class I bHLH transcription factor, such as E47. These dimers can bind to DNA regulatory sequences called E boxes (CAnnTG), inducing transcription of target genes (Massari and Murre 2000).

In the inner ear, afferent neurotransmission occurs through the release of an excitatory amino acid, probably glutamate, at ribbon synapses in inner hair cells onto afferent dendrites of eighth nerve fibers (Raphael and Altschuler 2003). Afferent excitation is modulated by the central nervous system through an efferent feedback, both onto afferent dendrites to inhibit firing and onto outer hair cells to dampen organ of Corti vibration (Raphael and Altschuler 2003). The second pathway, which modulates outer hair cells' role in amplification and tuning of acoustic signals, is especially important in auditory processing (Cooper and Guinan 2006; Lustig 2006). Acetylcholine (ACh) is a key neurotransmitter of the efferent system.

Nicotinic acetylcholine receptors (nAChR) are pentameric ligand-gated ion channels which are found in muscle at the neuromuscular junction, and in the peripheral and central nervous systems. Only two nicotinic subunits have been described in the inner ear hair cells: α9 (*Chrna9*) and α10 (*Chrna10*) (Elgoyhen *et al.* 1994, 2001). When expressed in *Xenopus laevis* oocytes, heteromeric receptors are formed that have many of the biophysical characteristics of the native hair cell nAChRs (Elgoyhen *et al.* 2001; Gomez-Casati *et al.* 2005), suggesting that α9 and α10 heteromultimers constitute the nAChRs of hair cells.

In this study, we found that the α1 nicotinic receptor subunit (*Chrna1*), which is a muscle-type nAChR subunit, is also expressed in the inner ear hair cells, as well as the γ (*Chrng*) subunit. These data lead us to propose that another type of nAChR is present in hair cells from embryonic stage E13.5 to post-natal stage P4. Moreover, we demonstrated that *Chrna1* transcription is under the control of ATOH1 *in vitro*.

Materials and methods

All primer used are summarized in Table 1.

Animal procedures

OF1 and CD1 mice were purchased from Charles River and dissected for *in situ* hybridization or RNA extraction. *Atoh1* knock-out and *Atoh1*-green fluorescent protein (GFP) mice were previously described (Bermingham *et al.* 1999; Lumpkin *et al.* 2003). Animal procedures were approved by the Standing Committee on Animals (Harvard Medical School), the Comité Régional d'Ethique pour l'Expérimentation Animale (France) and the National Institute of Health guide for the care and use of Laboratory animals (NIH Publications No. 80-23) revised 1978 (Argentina).

The *Atoh1* knock-out mice or embryos were genotyped using the *Atoh1* RT-PCR primers described below and the *lacZ* primers from the Jackson Laboratory web site. Thirty-five amplification cycles were performed with an annealing temperature of 58°C using both primer pairs in the same template. Loading on a 1.5% agarose gel allowed visualization of the 496 bp *Atoh1* and/or 315 bp *LacZ* bands.

Microarray expression analysis

Utricular maculas were dissected from eight litters of E18.5 *Atoh1* knock-out embryos. Total RNA extraction and labeled cRNA synthesis were performed as recommended by Affymetrix (small sample target labeling assay version II) using 50 ng of utricle RNA. The experiment was performed three times, two of them being totally independent and the third experiment only partially (starting from the first cycle of previously synthesized cRNA).

The hybridization to Affymetrix mouse MG-U74v2 chips was performed at the core facility of the Harvard Medical School. The images were analyzed using the Affymetrix Microarray Suite 5.0.0.032 software with a global scaling factor of 500 to acquire the target intensity. Fold changes and *p*-values were determined for the three experiments in comparison analysis. Only the genes with an increase call, a signal log ratio ≥1 (i.e., signal increased at least twofold) and a change p-value < 0.001 were considered.

Purification of hair cells and supporting cells by fluorescence-activated cell sorting (FACS)

Atoh1-GFP mouse pups were killed by decapitation. The inner ear capsules were removed and collected in Dulbecco's modified Eagle's medium-F12 (DMEM-F12) (HyClone, Logan, UT, USA). Utricles were dissected from the inner ears and then incubated in 0.5 mg/mL thermolysin (Sigma, St. Louis, MO, USA) in DMEM-F12 at 37°C for 35 min. The sensory epithelia were teased away from the stroma tissue with forceps and collected in a 35/10 mm tissue culture dish. The epithelia were triturated for 30–40 times in 0.25% trypsin-EDTA (Invitrogen, Carlsbad, CA, USA). One volume of trypsin inhibitor (Worthington, Lakewood, NJ, USA) was added to complete the dissociation, and the dissociated cells were then transferred to 1 mL CMF-PBS (Mediatech, Herndon, VA, USA) for sorting. The cells were sorted on a Becton Dickinson DiVa cell sorter (Franklin Lakes, NJ, USA). *Atoh1*-GFP+ hair cells comprised 25–30% of total cells. Sorted cells were collected in RN easy lysis buffer (RLT buffer); (Qiagen, Valencia, CA, USA) directly for RNA extraction to prevent cell loss.

Reverse transcription-polymerase chain reaction, semi-quantitative RT-PCR

Stably transfected osteosarcoma cells were grown in DMEM with and without tetracycline (TET) for 0, 2, 4, 6 or 8 h before extraction for time-course analysis of target genes expression. Cochleae and utricles plus saccules were dissected from OF1 mice or from wild-type, heterozygous or homozygous *Atoh1* knock-out littermates. RNA extractions were performed using Trizol reagent (Invitrogen).

Reverse transcriptase reactions were performed using Superscript II (Invitrogen), and PCR reactions using Taq polymerase (Invitrogen).

Table 1 Primer sets used in this study

	Forward	Reverse	Size (bp)
PCR *Atoh1*–/– genotyping			
LacZ	atcctctgcatggtcaggtc	cgtggcctgattcattcc	315
Atoh1	same as for RT-PCR	same as for RT-PCR	516
RT-PCR			
Human *GAPDH*	cggggctctccagaacatcat	acctttgacgctggggctgg	299
Mouse *Gapdh*	gatgcctgcttcaccaccttcttg	gcagaaggggcggagatgatgac	413
Human *CHRNA1*	tccgtgacctattcctgct	agtgctgtgcccttgattg	265
Mouse *Chrna1*	ctgggcacctggacctatga	cgtccatcatcatcaccgtc	444
Mouse *Chrng* (Yamane *et al.* 2002)	gatgcaatggtgcgactatcgc	gcctccgggtcaatgaagatcc	360
Mouse *Chrnd* (Drescher *et al.* 1995)	ctcaccctctccaacctc	gcggcggatgataaggtagaa	561
Mouse *Chrnb1*	gaccgactacaggttaagc	ccaacagcagcaagaacac	635
Mouse *Chrne*	ggacactgtcaccatcacc	gagcacgatgacgcaattca	841
Human *ATOH1*	cgcaatgttatcccgtcgtt	aaacttcgcctcggtcccac	459
Mouse *Atoh1*	agggtgagctggtaaggaga	cttctcaggcccagcttcc	516
FACS-sorted cells RT-PCR			
Mouse *Chrna1* set 1	tcaccgtcatcgtcatcaacacac	cccgatgagacacaccagcataaa	391
Mouse *Chrna1* set 2	accagcccgacctgagtaacttcat	gtgcttgatcagcggagagtgaaa	619
Mouse *Lhx3*	accaacttgagccttgtcccttca	gcgatgaagcaaggcgttactgtt	539
Mouse *Gapdh*	gtggccaaggtcatccatgacaac	catgaggtccaccaccctgttgct	506
Plasmid constructs			
Mouse *Atoh1* cDNA *EcoR*I/*Xba*I	ctgcagaattcatcagaccttgcagaagagacaggaag	accctctagaggtgcagggatatttgtcacgggct	1257
Mouse *Atoh1* cDNA HA-*Not*I		agtggcggccgcttcagctagcgtaatctggaacatcgtat gggtatccactggcctcatcagagtcactgtaatgagag	1173
Human *CHRNA1* promoter	cttttcatttctgctcttgaacca	agtgagaagcacaggccaccact	1927
In situ hybridization probes			
Chrna1	ctgggcacctggacctatga	tgctcacacggctgtattct	1336
Chrna10	atgtgaccctggaggtg	aggatcagctggaagacg	688
Chrng	gtcaatgtcagcctgaagcttacc	cgggatacagctctacaaacagca	1477
EMSA probes			
Probe P	agggcagcccagctgtcgctcccacaa		
Probe B	tcccacaaacaggtggtgtaaaacaat		
Probe PB	gggcagcccagctgtcgctcccacaaacaggtggtgtaaaa		
Probe P Mut	agggcagcccTgcAgtcgctcccacaa		
Probe B Mut	tcccacaaacTggAggtgtaaaacaat		
Probe PB MutP	gggcagcccTgcAgtcgctcccacaaacaggtggtgtaaaa		
Probe PB MutB	gggcagcccagctgtcgctcccacaaacTggAggtgtaaaa		
Probe PB MutPB	gggcagcccTgcAgtcgctcccacaaacTggAggtgtaaaa		

Amplicon sizes are indicated in base pair.

Plasmid constructs

The *Atoh1* coding sequence is intronless, therefore the cDNA sequence was cloned from genomic mouse DNA using the *EcoR*I/5′ and 3′UTR/*Xba*I primers. The PCR products were double-digested by *EcoR*I and *Xba*I, and cloned into the *EcoR*I/*Xba*I digested pCMV-sport6 expression vector. The *Atoh1* sequence was also amplified using the same *EcoR*I/5′ primer and a 3′UTR-HA/*Not*I primer, first cloned in the *EcoR*I/*Not*I sites of pTracer-CMV2 plasmid then cut by *EcoR*I/*Xba*I and subcloned between the *EcoR*I/*Xba*I sites of the pCMV-sport6 and pUHD10-3 vectors.

The E47 cDNA inserted in pCMV-sport6 expression vector was purchased as I.M.A.G.E clone #4505427. Its amino-acid sequence contains a single difference with the published amino-acid sequence of E47. As no evidence was obtained from public databases that this change may be a polymorphism, the sequence was corrected by site-directed mutagenesis (Quick-change, Stratagene, Hogehilweg, The Netherlands).

The 2 kb *CHRNA1* promoter construct was generated by PCR amplification using human genomic DNA (Boehringer) as template. Standard PCR reactions were performed using the human *CHRNA1* promoter primers. *Sal*I restriction enzyme sites were included in 5′ of forward and reverse primers. The PCR product was cloned into the luciferase reporter vector pXP1 [GenBank GI:3929277; Nordeen (1988)] linearized with the same enzyme. The 260 bp proximal promoter was generated using a *Bgl*II restriction site into the promoter. The resulting fragment was cloned into pXP1 previously digested by *Bgl*II and *Sal*I. The constructs with mutated E boxes were obtained by site-directed mutagenesis according to the

manufacturer's instructions (Quick-change, Stratagene). The E box E_P sequence was mutated CTgcAG instead of CAgcTG, and the E box E_B sequence was mutated CTggAG instead of CAggTG.

For *in situ* hybridization, the probes were cloned into the pCRII-Topo vector (Invitrogen) after amplification from mouse cochlear cDNA.

Cell culture transfection, luciferase assays and nuclear extracts: The stable TET-off system in U2OS cells (human osteosarcoma) (Lee *et al.* 1999) was obtained by transfection of the mouse *Atoh1* coding sequence fused to an HA tag in the pUHD10-3 vector. The cells were grown in DMEM supplemented with 10% fetal calf serum and hygromycine (0.4 ng/mL), with or without TET (1 μg/mL). HeLa and human embryonic kidney (HEK)293 cells were grown in DMEM supplemented with 10% fetal calf serum. Transfection and luciferase assays were carried out in the TET-off system, in HeLa cells and in HEK293 cells as previously described (Papin *et al.* 2003). We used Lipofectamine (Invitrogen) to transfect 3×10^5 HeLa cells, 4.5×10^5 HEK293 cells, or 4×10^5 osteosarcoma cells. Cell extracts were prepared and assayed with the luciferase assay system (Promega). Osteosarcoma-cell transfection medium was supplemented with TET (1 mg/mL), which was removed 3 h after the beginning of transfection. Each condition was performed in duplicate and results presented here are the mean of three or more experiments.

Nuclear extracts for electrophoretic mobility shift assay (EMSA) were prepared in HeLa cells as previously described (Papin *et al.* 2003), and characterized by western blot. All cell lines were free of mycoplasma infections.

Immunofluorescence

Osteosarcoma cells were cultured on glass coverslips. Cells were washed in PBS pH 7.4 and fixed in formaldehyde for 5 min at 25°C. Non-specific binding sites were blocked with PBS 0.1% Triton 8% normal goat serum for 1 h at 25°C. Cells were then incubated with primary antibody (anti-HA (Roche, Basel, Switzerland) 1 : 200, anti-ATOH1 (gift from J.E. Johnson 1 : 250) diluted into the blocking solution overnight at 4°C. They were incubated with respectively anti-mouse IgG (whole molecule)–FITC and anti-rabbit IgG (whole molecule)-Cy3 secondary antibody (Sigma–Aldrich, St. Louis, MO, USA), in the blocking solution for 1 h at 25°C, mounted in Vectashield medium containing DAPI (Vector Laboratories, Burlingame, CA, USA). Fluorescence images of transfected cells were then examined with a Leica DMR epifluorescence microscope (Wetzlar, Germany).

Western blot

Nuclear extracts were denatured for 10 min at 70°C. The proteins were loaded on 10% acrylamide sodium dodecyl sulfate gels and then electrotransfered onto polyvinylidene difluoride membranes (Amersham Biosciences, Uppsala, Sweden). The proteins were immunodetected by monoclonal anti-mouse MATH1/ATOH1 (Hybridoma bank) and affinity-purified rabbit polyclonal anti-E47 (N-649, Santa Cruz Biotechnology, Santa Cruz, CA, USA) antibodies, followed by horseradish peroxidase-conjugated anti-mouse or anti-rabbit IgG, and then visualized by chemiluminescence with the ECL + kit (Amersham Biosciences), according to the manufacturer's instructions. The chemiluminescence was detected by autoradiography. Antibodies were used at the following dilutions: anti-MATH1, 1/200; anti-E47, 1/200; anti-mouse-HRP, 1/50 000. anti-rabbit-HRP, 1/50 000.

Electrophoretic mobililty shift assay

Electrophoretic mobility shift assays were performed as previously described (Ben-Porath *et al.* 1999). Probes were double-stranded DNA oligonucleotides, end-labeled with [γ-^{33}P]-dCTP and the large fragment of DNA polymerase I (Invitrogen). Binding reactions were carried out for 45 min on ice using 20 μg of nuclear extracts, 0.5 ng of labeled probe, and 2 μg dI/dC in binding buffer. Supershifts were obtained adding 2 μg anti-HA antibody (Roche). Competition assays were performed by adding 1000-fold molar excess of unlabeled oligonucleotides. DNA-protein complexes were separated by electrophoresis on a cold 5% polyacrylamide gel in 0.5× tris-borate-EDTA (TBE) at 120 V. Gels were dried and analysed by Phosphorimager and Imagequant v5.2 (Molecular Dynamics). EMSA probes sequences are indicated in Table 1. When E boxes were mutated, oligonucleotide sequences included the same modifications as described in plasmid constructs.

Non-radioactive *in situ* hybridization

Inner ears of CD1 embryos and mice were collected at stages ranging from E13.5 to P7, fixed in 4% formaldehyde and cryosectioned (7- to 10-μm-thick frozen sections). *In situ* hybridizations were performed as previously described (Corey *et al.* 2004), with minor modifications : the hybridization solution contained 5X SSC, 50% formamide, 0.2 mg/mL yeast tRNA, 100 μg/mL heparin, 1X Denhardt's solution, 0.1% Tween 20 and 5 mmol/L EDTA, and hybridization was performed at 68°C.

Expression of recombinant receptors in *Xenopus laevis* oocytes

The constructs used were previously described and proved to be functional (http://www.salk.edu/labs/mnl-h/reagents.html; (Elgoyhen *et al.* 1994; Garcia-Colunga and Miledi 1999; Elgoyhen *et al.* 2001)). Capped cRNAs were *in vitro* transcribed from linearized plasmid DNA templates using the mMessage mMachine T7 Transcription Kit (Ambion Corporation, Austin, TX, USA) in the case of rat α9 and α10 and SP6 in the case of mouse α1, β1, γ and δ. The maintenance of *Xenopus laevis* as well as the preparation and cRNA injection of stage V and VI oocytes has been described in detail elsewhere (Katz *et al.* 2000). Electrophysiological recordings were performed 2–6 days after cRNA injection under two-electrode voltage clamp with an OC-725B oocyte clamp (Warner Instruments, Hamden, CT, USA). Both voltage and current electrodes were filled with 3 mol/L KCl, and had resistances of 1–2 MΩ. Data were analyzed using ClampFit from the pClamp 6 software (Axon Instruments Corp., Union City, CA, USA). During electrophysiological recordings, oocytes were continuously superfused (~10 mL/min) with normal frog saline comprising (mmol/L): 115 NaCl, 2.5 KCl, 1.8 $CaCl_2$, and 10 HEPES buffer, pH 7.2. Drugs were applied in the perfusion solution of the oocyte chamber. Only where stated, oocytes were incubated with the Ca^{2+} chelator 1,2-bis(2-aminophenoxy)ethane-*N*,*N*,*N*′,*N*′-tetraacetic acid-acetoxymethyl ester (BAPTA-AM, 100 μmol/L) for 4 h prior to electrophysiological recordings. Oocytes were clamped at a holding potential of −70 mV.

Current–voltage (*I–V*) relationships were obtained by applying 2-s voltage ramps from −120 to +50 mV from a holding potential of –70 mV 5 s after the peak response to ACh. Leakage correction was

performed by digital subtraction of the *I–V* curve obtained by the same voltage ramp protocol prior to the application of ACh. Generation of voltage protocols and data acquisition were performed with a Digidata 1200 and the pClamp 6.1 or 7.0 software (Axon Instruments Corp., Union City, CA, USA). Data were analyzed using ClampFit from the pClamp 6.1 software (Axon Instruments, Foster City, CA, USA).

Concentration–response curves to ACh were normalized to the maximal agonist response in each oocyte. The mean and standard error of the mean of peak current responses are represented. Agonist concentration–response curves were iteratively fitted with the equation:

$$I/I_{max} = A^n/(A^n + EC_{50}^n)$$

where I is the peak inward current evoked by the agonist at concentration A, I_{max} is the current evoked by the concentration of agonist eliciting a maximal response; EC_{50} is the concentration of agonist inducing half-maximal current response and n is the Hill coefficient.

Recordings from inner hair cells

Apical turns of the organ of Corti were excised from mice at postnatal day 4. Cochlear preparations were mounted under an Axioskop microscope (Zeiss, Oberkochen, Germany), and viewed with differential interference contrast using a 40× water immersion objective and a camera with contrast enhancement (Hamamatsu C2400-07, Hamamatsu City, Japan). Methods to record from IHC were essentially as described (Gomez-Casati *et al.* 2005). Briefly, IHCs were identified visually, by the size of their capacitance (7–12 pF) and by their characteristic voltage-dependent Na^+ and K^+ currents, including at older ages a fast-activating K^+ conductance (Kros *et al.* 1998). Some cells were removed to access IHCs, but mostly the pipette moved through the tissue using positive fluid flow to clear the tip. The extracellular solution was as follows (in mmol/L): 155 NaCl, 5.8 KCl, 1.3 $CaCl_2$, 0.9 $MgCl_2$, 0.7 NaH_2PO_4, 5.6 D-glucose, and 10 HEPES buffer; pH 7.4. The pipette solution was (in mmol/L): 150 KCl, 3.5 $MgCl_2$, 0.1 $CaCl_2$, 10 BAPTA, 5 HEPES buffer, 2.5 Na_2ATP, pH 7.2. Glass pipettes (1.2 mm i.d.) had resistances of 7–10 MΩ. Cells were held at a holding potential of −90 mV. Solutions containing ACh or nicotine were applied by a gravity-fed multi-channel glass pipette (~150 μm tip diameter) positioned about 300 μm from the recorded IHC. The extracellular solution containing the drugs was similar to that described above, except that Mg^{2+} was omitted, and the Ca^{2+} concentration was lowered to 0.5 mmol/L (Gomez-Casati *et al.* 2005). Currents in IHCs were recorded in the whole-cell patch-clamp configuration using an Axopatch 200B amplifier, low-pass filtered at 2–10 kHz and digitized at 5–20 kHz with a Digidata 1200 board (Axon Instruments, Union City, CA, USA). Recordings were made at room temperature (22–25°C). Voltages were not corrected for the voltage drop across the uncompensated series resistance.

Results

Chrna1 is expressed in inner ear hair cells

Atoh1−/− mice are totally devoid of hair cells in both the cochlea and vestibular system (Bermingham *et al.* 1999). We assessed gene expression in the utricular epithelium of wild-type and *Atoh1*−/− embryos (stage E18.5) using the MG-U74v2 Affymetrix GeneChips. *Chrna1* (probe set 166790_at), encoding the α1 subunit of the nicotinic acetylcholine receptor, was scored as present in the wild-type utricle and absent in the *Atoh1*−/− utricle. Signal in the wild-type was much higher than in the *Atoh1*−/− utricle (average signal log ratio = 2.7).

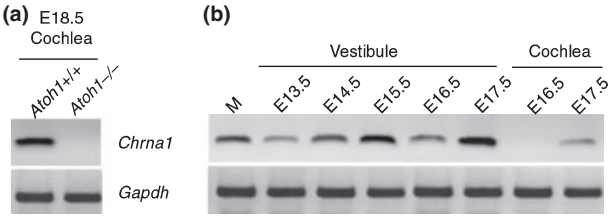

Fig. 1 *Chrna1* mRNA amplification in the inner ear. (a) *Chrna1* was expressed in wild-type cochlea although none was detectable in *Atoh1*–/– cochlea at E18.5. (b) Expression profile of *Chrna1* in the mouse vestibule (utricle and saccule) and cochlea determined by RT-PCR. Adult skeletal muscle (M) was used as a positive control. *Chrna1* was expressed from E13.5 onward in the vestibule and from E17.5 in the cochlea. The housekeeping gene *Gapdh* was used as an RT control. Messages were amplified with 35 cycles for *Chrna1* and 25 cycles for *Gapdh*.

To complement the microarray results, we used RT-PCR to assess the expression of *Chrna1* at E18.5 in the *Atoh1*$^{+/+}$ and *Atoh1*−/− cochlea and could not detect *Chrna1* in the *Atoh1*−/− cochlea (Fig. 1a). We then performed RT-PCR on the cochlea and vestibule at different stages of mouse early development. *Chrna1* begins to be detectable from E13.5 in the vestibule and E17.5 in the cochlea (Fig. 1b), following hair cell fate determination in each organ.

We analyzed the cellular expression of *Chrna1* in the mouse inner ear by *in situ* hybridization. On each head section, staining was observed in skeletal muscle and considered as the positive control (data not shown). In the inner ear, we found that *Chrna1* expression is restricted to hair cells of both the cochlear and vestibular sensory epithelia. Importantly, no expression was detected in the ganglia. *Chrna1* was detected as early as E18.5 in the cochlear inner and outer hair cells (Fig. 2a), and as early as E15.5 in the utricle, saccule and cristae ampularis (Fig. 2b and data not shown). *Chrna10* was used as a control probe for hair cell labeling. No signal was observed using the corresponding sense probes (data not shown).

To confirm that *Chrna1* expression is restricted to hair cells in the vestibule, we performed RT-PCR on FACS-sorted utricular hair cells from *Atoh1*-GFP mice. The use of two different sets of primers for *Chrna1* showed that this transcript, as well as the hair-cell specific gene *Lhx3,* is amplified only in GFP-positive cells at E16.5 (Fig. 2c) and E17.5 (data not shown).

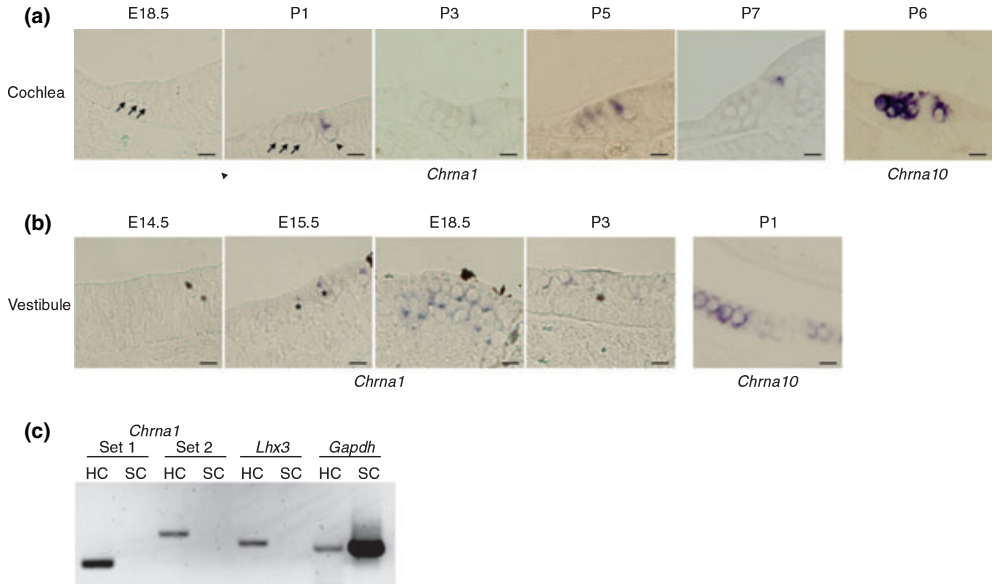

Fig. 2 *In situ* hybridization for *Chrna1* in mouse inner ear sensory epithelia from E14.5 to P7. (a) In the organ of Corti, *Chrna1* expression was restricted to the inner (arrowheads) and outer hair cells (arrows). mRNA was first detected at E18.5 in the bottom of hair cells.(b) In the vestibular epithelia, *Chrna1* expression was restricted to the hair cells (a few of them designated by asterisks). It was expressed from E15.5 and continued through P3 in the utricle and saccule. *Chrna10* was used as a control probe for hair cell labeling. Scale bars: 10 μm. (c) *Chrna1* mRNA amplification in FACS-sorted utricular hair cells. Two different sets of primers for *Chrna1* showed that it was expressed only in GFP^+ cells (hair cells; HC) and not in GFP^- cells (supporting cells; SC). *Lhx3* was used as a positive control for hair-cell-specific expression. The housekeeping gene *Gapdh* was used as an RT control. Messages were amplified with 35 cycles for *Chrna1* and *Lhx3* and 25 cycles for *Gapdh*.

ATOH1 induces expression of *Chrna1*

Four muscle class II bHLH transcription factors (MYOD, MYF-5, myogenin, and MYF-6), called myogenic regulatory factors (MRFs), are implicated in the activity-dependent regulation of the muscular nAChR subunits, including *Chrna1* (α1) (Piette *et al.* 1990; Prody and Merlie 1991; Liu *et al.* 2000; Wang *et al.* 2003; Zhao *et al.* 2003). Together, the specific hair-cell localization of *Chrna1*, its absence of expression in *Atoh1*−/− mice, and its transcriptional activation by other bHLHs (MRFs) suggested that the expression of *Chrna1* in hair cells is regulated by ATOH1. To test this hypothesis, we set up a TET-off system in osteosarcoma cells stably transfected with *Atoh1*-HA tagged, after verifying the lack of endogenous expression of ATOH1 in these cells (data not shown). Immunofluorescence using antibodies to the HA tag or to ATOH1 showed that the stably transfected cells express ATOH1 as soon as 2 h after removing TET (Fig. 3a, data not shown). We used semi-quantitative RT-PCR to assess the expression of *CHRNA1* at 2, 4, 6, and 8 h after removing TET (Fig. 3b). With TET present, ATOH1 expression is inhibited and the *CHRNA1* mRNA is only faintly amplified (Fig. 3b, TET+). When ATOH1 is induced (TET-), *CHRNA1* is over-expressed as early as 2 h, with stronger amplification 8 h after the beginning of ATOH1 expression. These data indicate fairly direct regulation by ATOH1.

ATOH1 activates *CHRNA1* expression through its promoter

Basic-helix-loop-helix transcription factors, such as ATOH1 act through regulatory sequences called E boxes (CAnnTG). Analysis of the promoter sequence of *CHRNA1* was performed using ClustalW (EMBL-EBI) and DNA block aligner (EMBL-EBI) between human (NM_000079, NT_005403.16), mouse (NM_007389, NT_039207.7) and chicken (NM_204816.1, NW_001471729). The proximal promoter (GenBank Z82984) contains two highly conserved E boxes named E_P and E_B (Fig. 4) (Piette *et al.* 1990). We cloned the 2 kb promoter region and inserted it in front of a luciferase reporter gene. When this construct was transfected in the TET-off model (Fig. 5a), a sixfold increase of the luciferase activity was detected after induction of ATOH1 expression (Fig. 5a, lane 2). Similar results were obtained with a 260 bp construct containing the minimal region of the proximal promoter with the two E boxes (lane 3). When either E_P or E_B was mutated, the induction was strongly reduced (lanes 4 and 5) and induction was totally lost when both E_P and E_B were mutated, either on the proximal promoter (lane 6) or the 2 kb construct (lane 7).

These results were confirmed in other cell types that do not express endogenous ATOH1 (HeLa, Fig. 5b; HEK293, data not shown). When only ATOH1 was co-transfected with the 2 kb promoter, it stimulated *CHRNA1*-mediated luciferase

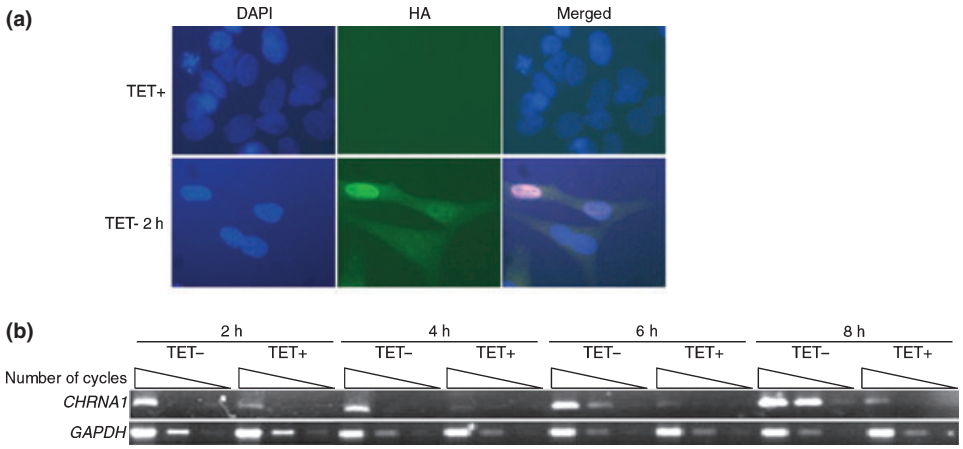

Fig. 3 Semi-quantitative RT-PCR of human *CHRNA1* under the control of ATOH1 in the TET-off system. (a) Immunofluorescence showing the expression of ATOH1-HA tagged in U2OS cells 2 h after removing TET. Cells were co-stained with 4′,6-diamidino-2-phenylindole (blue) and anti-HA (green). (b) *CHRNA1* expression in the presence (TET-) or absence (TET+) of ATOH1. The number of hours after the beginning of expression of ATOH1 is indicated. For each time point, we performed 30, 35, and 40 cycles of PCR. *CHRNA1* expression was up-regulated as early as 2 h after the induction of ATOH1 expression (TET-). The housekeeping gene *GAPDH* was amplified with 15, 20 and 25 cycles.

```
Human   GACTACTGGT GCATTTAAAA TATAATGCAG TTCATACTCA GCTT.GTCAA
Mouse   GACTCATGAT CTATGTAGAC TCTCAGACAC TTTACATCTA GT......AA
Chicken GATGTCTGTT GTGTGGGGCT TTTTTTAACC ACAACTCACA GTGCCGCTCA

Human   GGGTA.AGCA ATT....GTG TAAAGTGAGG CATATCTGTA ATGGTGTACA
Mouse   GAGTATAGCG ATC....ATG TTAAGCAAGG CACGTCTGTG ..........
Chicken GAAAAAAACG ATCTTTGGTG AACAGTAGGA GCCATCTGAG ....CGGTGC

Human   GTCCCAGTAA CTCCCTGGGC TCCAGG.GCT GAGG.GCAGC CCAGCTGTCG
Mouse   GCCACAG.AA GGCCCCAAGC TTTGAG.GCT GTGG.GCAGC TCAGCTGTCA
Chicken GACGCATTGT GCTCCCATTC CACAGCCGCT GTGGCGGCCC TCAGCTGTCA
                                                   EP

Human   CTCCCACAAA CAGGTGGTGT AAAACAATAG CTCTAGTGAG CCGACTCGCT
Mouse   TGCGGGCACA CAGGTGATGT AAGACAATAG CTGTGG..AG TCAGCTGGCT
Chicken TGCCTG.GAA CAGGTGGTGT AAGGCAAT.. CCCTGGGCAG CCG...TGCT
            EB                                        +1

Human   TTCCAAACCC TCCAGCAGAC AAGCACCC.. AGCCAGAGTG CCAGTGAGAA
Mouse   TCCAAGG... .CCAGCAGCC AAGCTCCCTA AGCCAGGGTG .....GAGTA
Chicken CCCCG..... .CCCCCCCCC GGGCC..... GACCTTAAAG .....GCGCT

Human   GCACAGGCCA CCACTCTGCC CTGGTCCACA CAAGCTCCGG TAGCCCATGG
Mouse   GGACCGGC.A GCAAGCCGCT GGCGGCCACA GCGGCACCCA CAGCCCATGG
Chicken GCGTGTGCCC TGGCTCCGCC GT.GCTGAGA GGAGCGGGCT CAGGTGATGG
```

Fig. 4 ClustalW alignment of the proximal promoter of *CHRNA1*. E boxes E_P and E_B (boxes) and the adjacent nucleotides are highly conserved between human, mouse, and chicken. Transcription start site (+1) and ATG (bold) are indicated.

expression (lane 2, white). This up-regulation may be due to the formation of heterodimers with an endogenous class I bHLH factor, or to the binding of ATOH1 homodimers on the promoter sequence. While E47 alone did not strongly influence the luciferase activity (lane 2, gray), the ATOH1-mediated luciferase induction was increased from 14- to 31-fold by co-transfection with E47 (lane 2, black), indicating a cooperative activity. The 260 bp construct showed an overall reduction of the induction by ATOH1/E47 from 31 to 9-fold (lane 3, black), indicating that other regulatory elements outside the 260 bp region are also involved in the synergistic interaction between ATOH1 and E47 in this cell type. Each E box mediates about half of this activity (fold induction was about 5 when E_P or E_B was mutated, lanes 4–5). The ATOH1/E47-induced expression of the luciferase activity was totally lost, either on the short promoter or the 2 kb promoter construct, when both E boxes were mutated (lanes 6–7).

ATOH1 regulates *CHRNA1* expression through direct binding to its promoter

In order to determine whether the complex ATOH1/E47 is able to bind to E_P and E_B *in vitro*, we used probes containing either one E box, or both, in EMSA (Fig. 6a, upper panel). Nuclear extracts used were verified by western blot before performing EMSAs (Fig. 6a, lower panel).

When the probe P was incubated with a nuclear extract containing both ATOH1 and E47, we observed a specific mobility shift (Fig. 6b left panel, lane 4, arrow), demonstrating the ability of ATOH1/E47 heterodimers to bind this

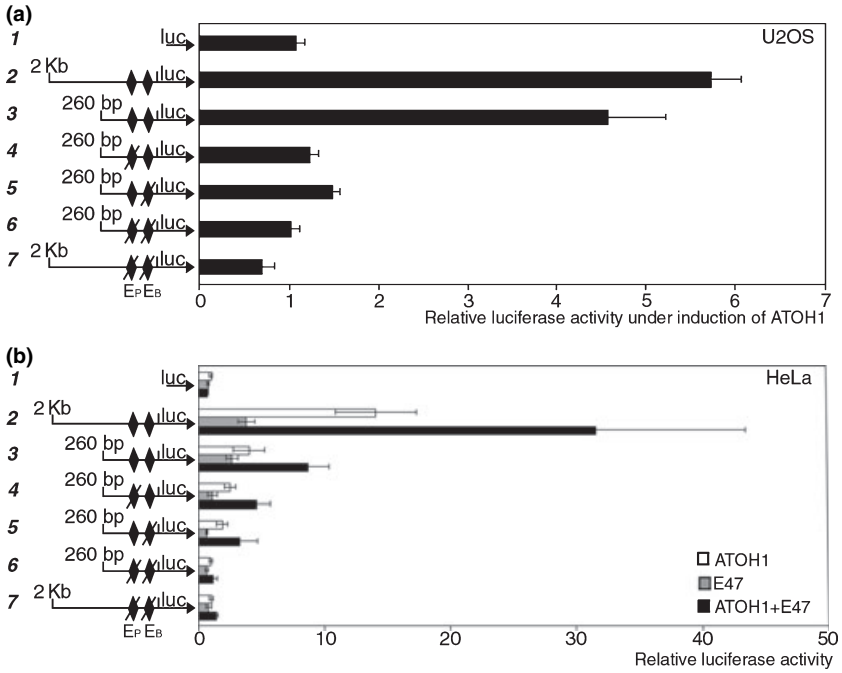

Fig. 5 *CHRNA1*-promoter-mediated luciferase activation by ATOH1. The reporter vector constructs used were: (1) empty luciferase vector, (2) *CHRNA1* promoter region 2 kb upstream of the transcription start site, (3) proximal promoter 260 bp upstream of the transcription start site, containing the two conserved E boxes, (4–6) the previous construct with either E_P, E_B, or both mutated, and (7) the 2 kb promoter with E_P and E_B mutated. (a) Transfection of the luciferase reporter constructs in U2OS cells and regulation of luciferase activity by induction of ATOH1 expression. (b) Co-transfection of the reporter constructs in HeLa cells with either *Atoh1*, *E47*, or both coding sequences. The luciferase activity of each construct was graphed as the fold increases over that of the cells without expression of ATOH1 (a) or empty expression vector (b).

sequence. The same result was obtained with an HA-tagged ATOH1 (lane 5). The formation of this complex was inhibited by an excess of unlabeled wild-type probe (lane 6). The shift does not occur with the E box E_P mutated in the same probe (data not shown). When the probe P was incubated with the nuclear extract containing only ATOH1, this shift was weakly reproduced because of the presence of endogenous E47 (lane 2). In addition, ATOH1 and E47 homodimers also shift the E-box probe to varying degrees [lanes 2 (white arrow) and 3 (arrowhead)], but the ATOH1/E47 protein-DNA complex appears to be the most favorable interaction, as already described (Helms *et al.* 2000). Very similar results were obtained with the probe B (Fig. 6b, right panel and data not shown).

In presence of the probe containing the two E boxes (probe PB), we observed the same shift as with single E boxes (Fig. 6c, left panel), but also an additional shift of higher molecular weight (arrows). It could result from the binding of two molecular ATOH1/E47 complexes on the probe, one on each E box. Consistent with this hypothesis, we observed the loss of the high molecular complex shift when only one E box was mutated on the PB probe (Fig. 6c, right panel, lanes 4 and 6), while the two shifts were lost when both P and B E boxes were mutated (lane 8).

Addition of an anti-HA antibody to the PB probe/ATOH1-HA/E47 complex resulted in a supershift (Fig. 6d, arrow) and a decrease in the intensity of the shift bands, indicating that ATOH1 is part of the shift complex. Therefore, the ATOH1-HA/E47 complex specifically binds the E_P and E_B of the *CHRNA1* promoter *in vitro*.

Electrophysiological recordings in *Xenopus* oocytes and hair cells

What is the function of α1 in hair cells? Two nicotinic AChR subunits, α9 and α10, are well known constituents of an ion channel mediating efferent feedback onto hair cells. In order to determine whether α1 might co-assemble with α9 and α10 *in vivo*, we asked if the co-expression of α1 with α9 and α10 in *Xenopus laevis* oocytes could modify their response to acetylcholine. Oocytes injected with α9 plus α1 cRNAs responded to 100 μmol/L ACh with very small inward currents (Fig. 7a, 10.6 ± 1.9 nA, $n = 6$) that did not differ in shape or amplitude from those recorded in α9-injected oocytes (Fig. 7b, 9.1 ± 1.5, $n = 4$). All nAChRs are activated by nicotine, except for α9 and α9α10 nAChRs (Elgoyhen *et al.* 1994, 2001). Oocytes injected with α9 and α1 nAChR subunits did not respond to nicotine (Fig. 7a), similarly to oocytes injected with α9 alone (Fig. 7b). The *I–V*

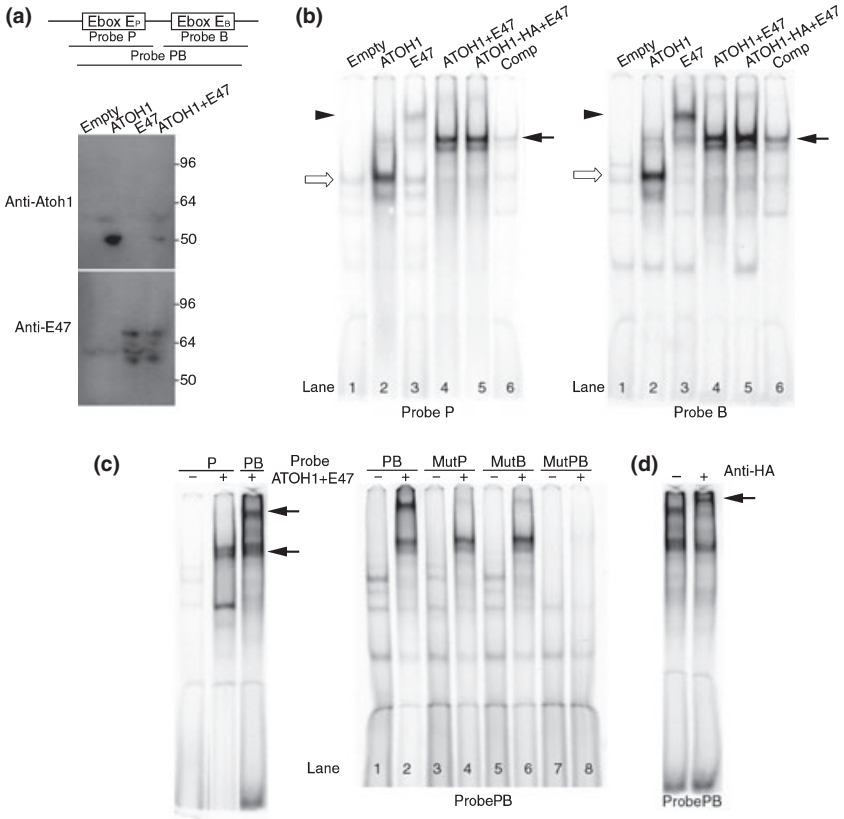

Fig. 6 Physical interaction between ATOH1/E47 and the two E boxes on the promoter of CHRNA1. (a) Upper panel: schematic representation of the proximal promoter of CHRNA1 probes used for EMSAs. Lower panel: immunoblot showing the expression of ATOH1 and E47 in nuclear extracts (NE) used for EMSAs. ATOH1 protein was detectable in NE of cells transfected with ATOH1 alone or together with E47. E47/E12 isoforms were detectable in NE of cells transfected with E47 alone or with both ATOH1/E47. (b) Left panel: interaction between probe P and NE containing none (empty vector), ATOH1, E47, ATOH1+E47 or ATOH1-HA-tagged+E47. The interaction between ATOH1/E47 (or ATOH1-HA/E47) and the probe results in a shift indicated by the black arrow. Black arrowhead and white arrow point out E47 and ATOH1 homodimers respectively. Competition (comp) was performed using an excess of cold probe. Right panel, same experiment with probe B. (c) Left panel: comparison of shifts obtained with probe P and probe PB (arrows), in the presence of ATOH1+E47 NE. The upper arrow shows a shift of higher molecular weight corresponding to the binding of two molecular complexes. Right panel: this shift was lost when one E box was mutated (MutP, MutB). Both upper and lower shifts were lost when the two E boxes were mutated (MutPB). For each probe, the first lane is with empty vector NE, and the second lane with ATOH1+E47 NE. (d) ATOH1 supershift (arrow) on the probe PB incubated with ATOH1-HA+E47 NE, and an anti-HA antibody. We could not observe this supershift replacing the anti-HA by an irrelevant antibody (data not shown). The unbound probe is not shown.

curve of α9 homomeric receptors has a unique signature: for voltages from +50 to −120 mV the curve is highly nonlinear, displaying a maximal inward current at around −60 mV. Inward currents elicited by ACh decreased between −60 and −25 mV, and were very small between −25 and +20 mV. Moreover, *I–V* curves performed from −120 to +50 showed very small currents at hyperpolarized potentials most likely due to divalent block (Katz *et al.* 2000). *I–V* curves obtained from α1α9–injected oocytes mimicked those of α9 homomeric receptors (Fig. 7a and b and (Elgoyhen *et al.* 1994)).

Co-injection of α1 with α10 cRNAs did not result in functional receptors (data not shown, $n = 18$), as for α10 alone. As previously reported (Elgoyhen *et al.* 2001), the co-injection of α9 with α10 nAChR subunits resulted in responses to ACh that were 20-fold larger than those with α9 homomeric receptors (Fig. 7d, 201 ± 63 nA, $n = 6$). Among nAChRs, the α9α10 receptor has the highest Ca^{2+} permeability, but the muscle nAChR has the lowest permeability to divalent cations (Vernino *et al.* 1992). As previously shown, currents elicited by the application of 100 μmol/L ACh to α9α10 expressing oocytes were reduced by approximately 88% after 4 h of incubation with the fast calcium chelator BAPTA-AM (Fig. 7d). The co-expression of α9α10 with α1 also resulted in currents of similar intensity (163 ± 20 nA, $n = 6$) that were also largely blocked by BAPTA-AM (99%, $n = 3$) (Fig. 7c), indicating that the ACh-evoked current had a high Ca^{2+} permeability similar to α9α10 nAChRs. To avoid the activation of Ca^{2+}-activated

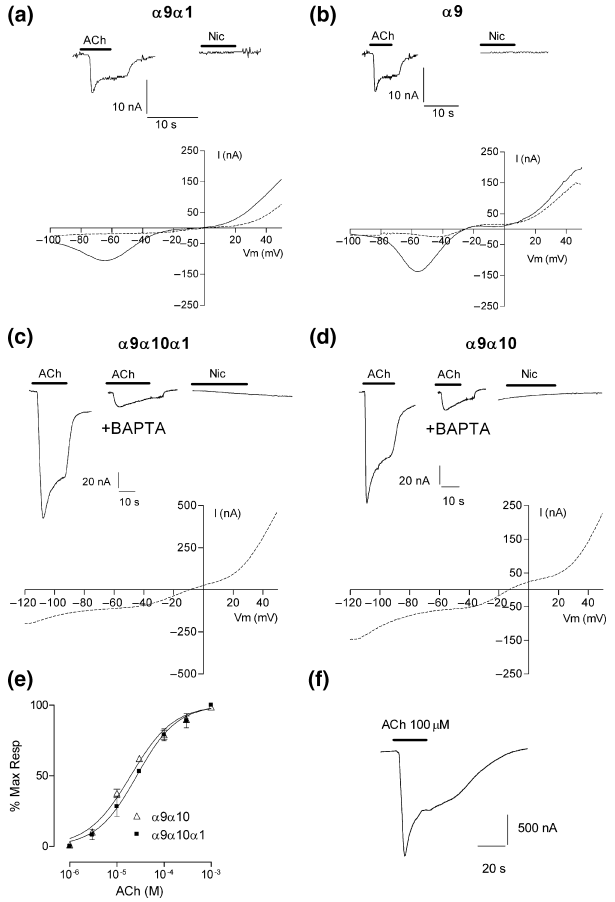

Fig. 7 Co-injection of α1 with α9 or with α9 and α10 cRNAs in *Xenopus* laevis oocytes. (a and b), upper panel, representative responses to either 100 μmol/L ACh or 100 μmol/L nicotine, of oocytes injected with α9 and α1 cRNAs (a, $n = 6$), and α9 only (b, $n = 4$). Lower panel, *I–V* curves were measured by applying a voltage ramp either from −120 to +50 mV (—) or from +50 to −120 (—). (c and d) Upper panel, representative responses to either 100 μmol/L ACh (in the absence and presence of BAPTA) or 100 μmol/L nicotine ($n = 6$), of oocytes injected with α9, α10 and α1 (c), and α9 and α10 (d). Lower panel, *I–V* curves were measured by applying a voltage ramp from −120 to +50 mV (in the presence of BAPTA). (e) Concentration-response curves to ACh (in the presence of BAPTA). Values represented are the mean and standard error of the mean of peak current obtained in 5–10 oocytes. Responses of each oocyte were normalized to the maximal current evoked by ACh. (f) Representative responses to 100 μmol/L ACh at a holding potential of −70 mV in oocytes injected with α1, β1, γ, and δ cRNAs.

Cl^- current, the subsequent experiments were performed in the presence of BAPTA. α9α10 receptors showed no response to nicotine and had a non-linear *I–V* curve (Fig. 7d). The response of α9α10 nAChR to ACh was concentration-dependent with an apparent affinity of 18.3 ± 0.6 μmol/L ($n = 10$) (Fig. 7e). The addition of α1 subunits did not modify the amplitude (Fig. 7c and d) (63 ± 15 nA, $n = 6$, compared to 70 ± 20, $n = 6$ in the presence of the α1 subunit) or the time course of responses to ACh, it did not change the apparent affinity for ACh (Fig. 7e) (23.6 ± 0.8 μmol/L, $n = 5$), it did not result in responses to nicotine, and it did not change the shape of the non-linear *I–V* curves from those of α9α10 alone (Fig. 7c and d, lower panels). As shown in Fig. 7f, the α1 construct did yield functional receptors when expressed with the β1, γ and δ cRNAs (2.3 ± 0.2 μA, $n = 5$).

As muscle-type nAChRs, but not α9α10, respond to nicotine (Elgoyhen *et al.* 2001; Beene *et al.* 2002), we asked whether nicotine can induce a current in cochlear hair cells. As shown in Fig. 8, IHCs at age P4 that did respond to ACh (218.97 ± 19.3 pA, 7 cells, 4 animals) did not respond to nicotine, thus suggesting the lack of muscle-type ($\alpha_2\beta\delta\gamma/\varepsilon$) nAChRs at this stage.

A novel type of nAChR in inner ear hair cells?

The observation that α1 does not change the electrophysiological properties of α9α10 suggests that α1 does not co-assemble with α9α10 receptor. Despite the insensitivity of IHCs to nicotine at P4, α1 may participate in another nAChR in hair cells at an earlier stage.

We therefore tested the expression of the other muscle-type nicotinic subunits by RT-PCR in the cochlea at embryonic stage E18.5 (Fig. 9). *Chrne* was not detected at this stage (data not shown), consistent with its expression in muscle where it replaces the fetal γ subunit in the adult-type nAChR. The β1, δ, and γ subunits, encoded by *Chrnb1*, *Chrnd*, and *Chrng* respectively, were all amplified in wild-type cochlea . The *Atoh1*−/− mice are a powerful tool to study hair-cell specific genes as they lack hair cells. Indeed, the expression of *Chrng* message was dramatically reduced in the cochlea of *Atoh1*−/− mice, suggesting that its expression may be hair-cell-specific.

Thus, we asked where and when *Chrng* is expressed in inner ear sensory epithelia. *In situ* hybridization showed that it is expressed only in vestibular hair cells as soon as E13.5 and in outer hair cell and IHC of the cochlea from E17.5 (Fig. 10). Its onset of expression is therefore close to that of *Chrna1*. By P4, *Chrng* is silenced at the base and mid-turn of the cochlea, while it is still expressed at the apex (Fig. 10b, data not shown). It totally disappears at later postnatal stages. Skeletal muscle fibers were used as a positive control (data not shown). Thus, two muscle-type nAChR subunits, *Chrna1* and *Chrng*, are expressed in hair cells of the inner ear sensory epithelia during embryogenesis.

Discussion

Hair cells are innervated by both afferent and efferent systems. Outer hair cells receive efferent axons from neurons located in the superior olivary complex of the brainstem and are part of a feedback loop that regulates sensitivity and frequency selectivity. Acetylcholine is one of the principal

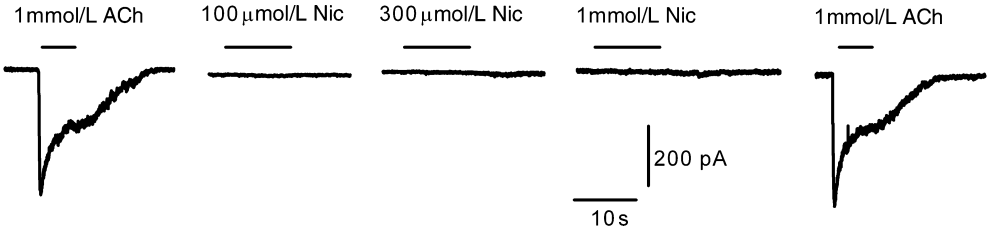

Fig. 8 Currents evoked by 1 mmol/L ACh in IHCs (first and last traces). Nicotine at 100 μmol/L, 300 μmol/L or 1 mmol/L (middle traces) failed to evoke any current. All experiments were carried out in postnatal day 4 IHCs voltage-clamped at −90 mV. The traces are representative of seven cells from four mice.

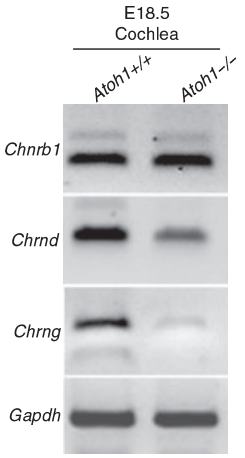

Fig. 9 Expression of muscle-type nAChR subunits by RT-PCR in the wild-type and *Atoh1*−/− mice at embryonic stage E18.5. The β1, δ, and γ subunits are expressed in wild-type mice cochlea. The β1- and δ-subunit expression did not significantly decrease in the mutant mice cochlea, whereas the γ message was dramatically down-regulated. Messages were amplified with 35 cycles except the housekeeping gene *Gapdh* with 25 cycles.

neurotransmitters of the inner ear efferent system. Among all the nAChR subunits described in the inner ear, only two, α9 (*Chrna9*) and α10 (*Chrna10*), have been thoroughly studied in hair cells (Elgoyhen *et al.* 1994, 2001; Housley *et al.* 1994; Drescher *et al.* 1995; Anderson *et al.* 1997; Luo *et al.* 1998; Morley *et al.* 1998; Luebke and Foster 2002). In this study, we show that two subunits of the muscle-type nAChR, α1 (encoded by *Chrna1*) and γ (encoded by *Chrng*), are also expressed at least transiently in the inner ear hair cells.

In skeletal muscle, two α1 subunits co-assemble with the β1, δ, and γ (embryonic) or ε (mature) subunits to form a functional heteropentameric acetylcholine receptor ($\alpha_2\beta\delta\gamma/\varepsilon$). Until now, no evidence of a functional heterodimerization of α1 with any other α nAChR subunit, such as α9 and/or α10, has been reported. Moreover, α1 monomers have a dramatically reduced half-life (2 h, compared to 13 h when assembled with the δ subunit) (Blount and Merlie 1990; Blount *et al.* 1990). Therefore, α1 is more likely to be rapidly degraded in *Xenopus* oocytes as it does not seem to co-assemble with α9 and α10 in our experiments. Thus, our results showing that α1 does not change electrophysiological properties of the α9α10 nicotinic acetylcholine receptor suggest that instead it collaborates with other subunits in hair cells.

The α1 subunit is stabilized through the association with γ or δ subunits. This association is a pre-requisite for generating functional receptors (Kurosaki *et al.* 1987; Liu and Brehm 1993). We show that the other muscular subunits β1, δ, and γ are also expressed in the cochlea at embryonic

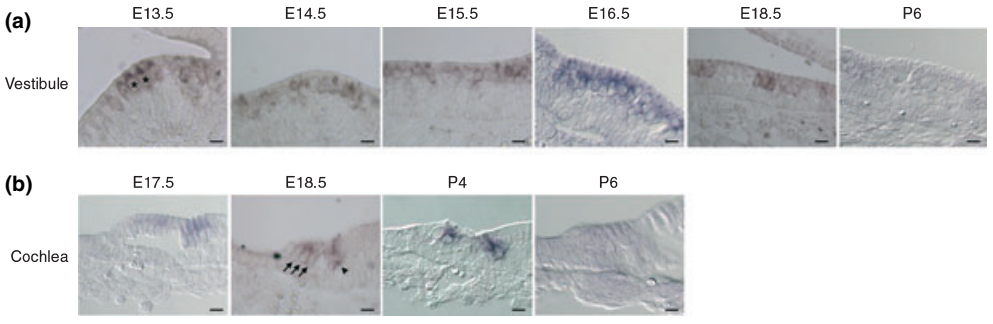

Fig. 10 *In situ* hybridization for *Chrng* in mouse inner ear sensory epithelia from E13.5 to P6. (a) In the vestibular epithelia, *Chrng* was expressed in the utricular and saccular hair cells (asterisk) from E13.5. (b) In the organ of Corti, *Chrng* expression was detected from E17.5 in inner (arrowhead) and outer (arrows) hair cells. At P4, *Chrng* was expressed only at the apex. It was silenced in both the cochlea and vestibule at P6. Scale bars: 10 μm.

stage E18.5. The dramatic decrease of *Chrng* expression we found in *Atoh1* mutant mice, combined with *in situ* hybridization, confirms that *Chrng* is expressed together with *Chrna1* in inner ear hair cells during embryogenesis and early post-natal stages. The mouse α1γ combination as been shown to result in functional receptors when injected in *Xenopus laevis* oocytes (Kurosaki *et al.* 1987; Liu and Brehm 1993). Furthermore, nAChR heterogeneity has been reported *in vivo* in vertebrate skeletal muscle, suggesting that muscle-type subunits can co-assemble in different ways according to the expressed subunits (Jackson *et al.* 1990; Sine and Claudio 1991). Together, the absence of changes in the electrophysiological properties of the α9α10 nAChR by coinjection with α1 in *Xenopus* oocytes, and the co-expression of the γ subunit in hair cells during embryonic stages, suggest that inner ear hair cells express a combination of muscle subunits that forms a α1γ-containing receptor distinct from the α9α10 receptor.

A α1γ-containing nAChR may participate in the efferent transmission between nerve fibers and hair cells. Dresher *et al.* tested the expression of the five muscle-type nAChR subunits in late postnatal mouse cochlea (P14-P18) and detected only β1 (Drescher *et al.* 1995). Before the onset of hearing (P12-P14), the efferent response could result from the synergy of several types of nAChR, including α9α10 cysteine-rich protein 3 (or Muscle LIM Protein) (Elgoyhen *et al.* 1994, 2001; Vetter *et al.* 1999; Sgard *et al.* 2002) and α1γ-containing receptors. Alternatively, the time-dependent expression of nAChRs also could play a key role in directing the innervation pattern of hair cells during early development. The expression profiles of the α1 and γ subunits are related to the arrival of efferent fibers in the sensory epithelia, and could be critical for early synaptic development in the cochlea and vestibule. The extinction of *Chrng* at P4 and the absence of nicotine response in IHC at this stage are indeed consistent with an embryological function. In muscle, temporary synaptic contacts are established during embryogenesis. Subsequently, the process of synapse elimination results in a reduction of polyneural innervation and establishment of the adult pattern of innervation (Sanes and Lichtman 1999). Also, embryonic synaptic specialization at non-terminal regions of axons temporarily form during axon pathfinding (Sheard and Duxson 1997). Interestingly, a gain-of-function mutation of the α1 subunit in zebrafish causes abnormal motor axonal extension and muscular degeneration (Lefebvre *et al.* 2004). The use of mutant mice in which the γ (fetal) subunit was replaced by an ε-like adult subunit showed abnormal branching of motor nerves and an altered distribution of neuromuscular synapses, suggesting that the γ subunit has an important role in directing the innervation pattern to ensure an orderly innervation of skeletal muscle (Koenen *et al.* 2005).

In differentiating muscle, the nAChR subunits are transcriptionaly regulated by myogenic regulatory factors (MRFs) (Olson 1990; Jia *et al.* 1992; Weintraub 1993). We showed that α1 is regulated by another bHLH factor, ATOH1. In the inner ear, ATOH1 is necessary and sufficient for hair cell development (Bermingham *et al.* 1999). Little is known about its molecular effects and few transcriptional targets have been described; these include its own enhancer (Helms *et al.* 2000), *Mbh1* (Saba *et al.* 2005) and *Nr2f6* (Krizhanovsky *et al.* 2006). So far, no direct ATOH1 downstream target has been characterized in the inner ear. Here, we show the *in vitro* transcriptional regulation of *Chrna1* by ATOH1 through direct binding on two E boxes located on the proximal promoter.

The timing of *Chrna1* expression (E13.5) is close to *Atoh1* in vestibular hair cells, consistent with a direct transcriptional activation *in vivo*. This regulation seems to be more complex in the organ of Corti : *Atoh1* begins to be expressed at E13.5 whereas *Chrna1* appears later (E17.5), indicating a requirement for other regulatory factors. Several studies have demonstrated a cooperative regulation between bHLH proteins (e.g., MASH1, MyoD) and other transcription factors (e.g., homeodomain proteins, LIM proteins, SOX or Brn family factors) to provide the tissue and timing specificity of expression (Bertrand *et al.* 2002; Westerman *et al.* 2003; Lu *et al.* 2004; Castro *et al.* 2006). Interestingly, there is such an example on the promoter of *Chrng*, between myogenin and cysteine-rich protein 3 (or muscle LIM protein) (Lu *et al.* 2004). Moreover, regulatory elements other than E_P and E_B have been described for the muscle chick *Chrna1* promoter (Bessereau *et al.* 1998). A reasonable speculation is that other factor(s) act as *cis*-regulatory element(s) of the α1 subunit gene in cochlear hair cells. However, the literature shows no transcription factor differentially expressed between cochlear and vestibular hair cells. The identification of other ATOH1 transcriptional targets will help to characterize the inter-regulation between transcription factors during hair cell development.

In summary, we have described for the first time the expression of two additional nAChR subunits, α1 and γ, in hair cells of the inner ear. Moreover, we showed the transcriptional regulation of *Chrna1* by ATOH1 *in vitro*. α1 and ATOH1 are expressed together in inner ear hair cells, leading to the possibility that ATOH1 also regulates *Chrna1* *in vivo*. In muscle, γ and α1 subunits start to be expressed under the control of another bHLH factor, MyoD (Piette *et al.* 1990; Prody and Merlie 1991; Charbonnier *et al.* 2003; Zhao *et al.* 2003). So, it seems possible that ATOH1 also activates the γ subunit expression in hair cells. The α1 subunit seems not to heteromultimerize with α9 and α10 subunits, but it may form a distinct type of nAChR in hair cells with the γ subunit and possibly other muscle subunit(s). We propose that these α1γ-containing nAChRs play a role during the development of efferent fibers in the inner ear sensory epithelia.

Acknowledgments

We want to thank M.E Gomez-Casati for her graphics help for the electrophysiology data, R. Palmer for technical assistance (U2OS cells), Dr J. Boulter for providing the mouse α1, δ, γ, and β1 cDNA clones, Dr Jane E. Johnson for the monoclonal rabbit anti-ATOH1 antibody and Dr H.Y Zoghbi for the *Atoh1−/−* mice. This work was supported by the Avenir project at INSERM, a grant from the NIH/NIDCD to DPC, a grant from the NIH/NIDCD (DC04546) to ZYC, an International Research Scholar Grant from the Howard Hughes Medical Institute and a Research Grant from ANPCyT and UBA (Argentina) to ABE. DS is a recipient of a INSERM/Ile de France and Fondation pour la Recherche Medicale fellowship. DPC is an Investigator, ABE is an International Research Scholar and VP was an Associate of the Howard Hughes Medical Institute.

References

Anderson A. D., Troyanovskaya M. and Wackym P. A. (1997) Differential expression of alpha2-7, alpha9 and beta2-4 nicotinic acetylcholine receptor subunit mRNA in the vestibular end-organs and Scarpa's ganglia of the rat. *Brain Res.* **778**, 409–413.

Barald K. F. and Kelley M. W. (2004) From placode to polarization: new tunes in inner ear development. *Development* **131**, 4119–4130.

Beene D. L., Brandt G. S., Zhong W., Zacharias N. M., Lester H. A. and Dougherty D. A. (2002) Cation-pi interactions in ligand recognition by serotonergic (5-HT3A) and nicotinic acetylcholine receptors: the anomalous binding properties of nicotine. *Biochemistry* **41**, 10262–10269.

Ben-Arie N., Bellen H. J., Armstrong D. L., McCall A. E., Gordadze P. R., Guo Q., Matzuk M. M. and Zoghbi H. Y. (1997) Math1 is essential for genesis of cerebellar granule neurons. *Nature* **390**, 169–172.

Ben-Porath I., Yanuka O. and Benvenisty N. (1999) The tmp gene, encoding a membrane protein, is a c-Myc target with a tumorigenic activity. *Mol. Cell. Biol.* **19**, 3529–3539.

Bermingham N. A., Hassan B. A., Price S. D., Vollrath M. A., Ben-Arie N., Eatock R. A., Bellen H. J., Lysakowski A. and Zoghbi H. Y. (1999) Math1: an essential gene for the generation of inner ear hair cells. *Science* **284**, 1837–1841.

Bermingham N. A., Hassan B. A., Wang V. Y., Fernandez M., Banfi S., Bellen H. J., Fritzsch B. and Zoghbi H. Y. (2001) Proprioceptor pathway development is dependent on Math1. *Neuron* **30**, 411–422.

Bertrand N., Castro D. S. and Guillemot F. (2002) Proneural genes and the specification of neural cell types. *Nat. Rev. Neurosci.* **3**, 517–530.

Bessereau J. L., Laudenbach V., Le Poupon C. and Changeux J. P. (1998) Nonmyogenic factors bind nicotinic acetylcholine receptor promoter elements required for response to denervation. *J. Biol. Chem.* **273**, 12786–12793.

Blount P. and Merlie J. P. (1990) Mutational analysis of muscle nicotinic acetylcholine receptor subunit assembly. *J. Cell Biol.* **111**, 2613–2622.

Blount P., Smith M. M. and Merlie J. P. (1990) Assembly intermediates of the mouse muscle nicotinic acetylcholine receptor in stably transfected fibroblasts. *J. Cell Biol.* **111**, 2601–2611.

Castro D. S., Skowronska-Krawczyk D., Armant O. *et al.* (2006) Proneural bHLH and Brn proteins coregulate a neurogenic program through cooperative binding to a conserved DNA motif. *Dev. Cell* **11**, 831–844.

Charbonnier F., Della Gaspara B., Armand A. S., Lecolle S., Launay T., Gallien C. L. and Chanoine C. (2003) Specific activation of the acetylcholine receptor subunit genes by MyoD family proteins. *J. Biol. Chem.* **278**, 33169–33174.

Cooper N. P. and Guinan Jr. J. J. (2006) Efferent-mediated control of basilar membrane motion. *J. Physiol.* **576**, 49–54.

Corey D. P., Garcia-Anoveros J., Holt J. R. *et al.* (2004) TRPA1 is a candidate for the mechanosensitive transduction channel of vertebrate hair cells. *Nature* **432**, 723–730.

Drescher D. G., Khan K. M., Green G. E., Morley B. J., Beisel K. W., Kaul H., Gordon D., Gupta A. K., Drescher M. J. and Barretto R. L. (1995) Analysis of nicotinic acetylcholine receptor subunits in the cochlea of the mouse. *Comp. Biochem. Physiol. C Pharmacol. Toxicol. Endocrinol.* **112**, 267–273.

Eatock R. A. and Hurley K. M. (2003) Functional development of hair cells. *Curr. Top. Dev. Biol.* **57**, 389–448.

Elgoyhen A. B., Johnson D. S., Boulter J., Vetter D. E. and Heinemann S. (1994) Alpha 9: an acetylcholine receptor with novel pharmacological properties expressed in rat cochlear hair cells. *Cell* **79**, 705–715.

Elgoyhen A. B., Vetter D. E., Katz E., Rothlin C. V., Heinemann S. F. and Boulter J. (2001) alpha10: a determinant of nicotinic cholinergic receptor function in mammalian vestibular and cochlear mechanosensory hair cells. *Proc. Natl Acad. Sci. USA* **98**, 3501–3506.

Fettiplace R. and Hackney C. M. (2006) The sensory and motor roles of auditory hair cells. *Nat. Rev. Neurosci.* **7**, 19–29.

Garcia-Colunga J. and Miledi R. (1999) Blockage of mouse muscle nicotinic receptors by serotonergic compounds. *Exp. Physiol.* **84**, 847–864.

Gomez-Casati M. E., Fuchs P. A., Elgoyhen A. B. and Katz E. (2005) Biophysical and pharmacological characterization of nicotinic cholinergic receptors in rat cochlear inner hair cells. *J. Physiol.* **566**, 103–118.

Helms A. W., Abney A. L., Ben-Arie N., Zoghbi H. Y. and Johnson J. E. (2000) Autoregulation and multiple enhancers control Math1 expression in the developing nervous system. *Development* **127**, 1185–1196.

Housley G. D., Batcher S., Kraft M. and Ryan A. F. (1994) Nicotinic acetylcholine receptor subunits expressed in rat cochlea detected by the polymerase chain reaction. *Hear. Res.* **75**, 47–53.

Izumikawa M., Minoda R., Kawamoto K., Abrashkin K. A., Swiderski D. L., Dolan D. F., Brough D. E. and Raphael Y. (2005) Auditory hair cell replacement and hearing improvement by Atoh1 gene therapy in deaf mammals. *Nat. Med.* **11**, 271–276.

Jackson M. B., Imoto K., Mishina M., Konno T., Numa S. and Sakmann B. (1990) Spontaneous and agonist-induced openings of an acetylcholine receptor channel composed of bovine muscle alpha-, beta- and delta-subunits. *Pflugers Arch.* **417**, 129–135.

Jia H. T., Tsay H. J. and Schmidt J. (1992) Analysis of binding and activating functions of the chick muscle acetylcholine receptor gamma-subunit upstream sequence. *Cell. Mol. Neurobiol.* **12**, 241–258.

Katz E., Verbitsky M., Rothlin C. V., Vetter D. E., Heinemann S. F. and Elgoyhen A. B. (2000) High calcium permeability and calcium block of the alpha9 nicotinic acetylcholine receptor. *Hear. Res.* **141**, 117–128.

Kawamoto K., Ishimoto S., Minoda R., Brough D. E. and Raphael Y. (2003) Math1 gene transfer generates new cochlear hair cells in mature guinea pigs in vivo. *J. Neurosci.* **23**, 4395–4400.

Koenen M., Peter C., Villarroel A., Witzemann V. and Sakmann B. (2005) Acetylcholine receptor channel subtype directs the innervation pattern of skeletal muscle. *EMBO Rep.* **6**, 570–576.

Krizhanovsky V., Soreq L., Kliminski V. and Ben-Arie N. (2006) Math1 target genes are enriched with evolutionarily conserved clustered E-box binding sites. *J. Mol. Neurosci.* **28**, 211–229.

Kros C. J., Ruppersberg J. P. and Rusch A. (1998) Expression of a potassium current in inner hair cells during development of hearing in mice. *Nature* **394**, 281–284.

Kurosaki T., Fukuda K., Konno T., Mori Y., Tanaka K., Mishina M. and Numa S. (1987) Functional properties of nicotinic acetylcholine receptor subunits expressed in various combinations. *FEBS Lett.* **214**, 253–258.

Lee S. B., Huang K., Palmer R. *et al.* (1999) The Wilms tumor suppressor WT1 encodes a transcriptional activator of amphiregulin. *Cell* **98**, 663–673.

Lefebvre J. L., Ono F., Puglielli C., Seidner G., Franzini-Armstrong C., Brehm P. and Granato M. (2004) Increased neuromuscular activity causes axonal defects and muscular degeneration. *Development* **131**, 2605–2618.

Liu Y. and Brehm P. (1993) Expression of subunit-omitted mouse nicotinic acetylcholine receptors in Xenopus laevis oocytes. *J. Physiol.* **470**, 349–363.

Liu S., Spinner D. S., Schmidt M. M., Danielsson J. A., Wang S. and Schmidt J. (2000) Interaction of MyoD family proteins with enhancers of acetylcholine receptor subunit genes in vivo. *J. Biol. Chem.* **275**, 41364–41368.

Lu P. Y., Taylor M., Jia H. T. and Ni J. H. (2004) Muscle LIM protein promotes expression of the acetylcholine receptor gamma-subunit gene cooperatively with the myogenin-E12 complex. *Cell Mol. Life Sci.* **61**, 2386–2392.

Luebke A. E. and Foster P. K. (2002) Variation in inter-animal susceptibility to noise damage is associated with alpha 9 acetylcholine receptor subunit expression level. *J. Neurosci.* **22**, 4241–4247.

Lumpkin E. A., Collisson T., Parab P. *et al.* (2003) Math1-driven GFP expression in the developing nervous system of transgenic mice. *Gene Expr. Patterns* **3**, 389–395.

Luo L., Bennett T., Jung H. H. and Ryan A. F. (1998) Developmental expression of alpha 9 acetylcholine receptor mRNA in the rat cochlea and vestibular inner ear. *J. Comp. Neurol.* **393**, 320–331.

Lustig L. R. (2006) Nicotinic acetylcholine receptor structure and function in the efferent auditory system. *Anat. Rec. A Discov. Mol. Cell Evol. Biol.* **288**, 424–434.

Massari M. E. and Murre C. (2000) Helix-loop-helix proteins: regulators of transcription in eucaryotic organisms. *Mol. Cell. Biol.* **20**, 429–440.

Morley B. J., Li H. S., Hiel H., Drescher D. G. and Elgoyhen A. B. (1998) Identification of the subunits of the nicotinic cholinergic receptors in the rat cochlea using RT-PCR and in situ hybridization. *Brain Res. Mol. Brain Res.* **53**, 78–87.

Nordeen S. K. (1988) Luciferase reporter gene vectors for analysis of promoters and enhancers. *Biotechniques* **6**, 454–458.

Olson E. N. (1990) MyoD family: a paradigm for development? *Genes Dev.* **4**, 1454–1461.

Papin S., Cazeneuve C., Duquesnoy P., Jeru I., Sahali D. and Amselem S. (2003) The tumor necrosis factor alpha-dependent activation of the human mediterranean fever (MEFV) promoter is mediated by a synergistic interaction between C/EBP beta and NF kappaB p65. *J. Biol. Chem.* **278**, 48839–48847.

Piette J., Bessereau J. L., Huchet M. and Changeux J. P. (1990) Two adjacent MyoD1-binding sites regulate expression of the acetylcholine receptor alpha-subunit gene. *Nature* **345**, 353–355.

Prody C. A. and Merlie J. P. (1991) A developmental and tissue-specific enhancer in the mouse skeletal muscle acetylcholine receptor alpha-subunit gene regulated by myogenic factors. *J. Biol. Chem.* **266**, 22588–22596.

Raphael Y. and Altschuler R. A. (2003) Structure and innervation of the cochlea. *Brain Res. Bull.* **60**, 397–422.

Riley B. B. and Phillips B. T. (2003) Ringing in the new ear: resolution of cell interactions in otic development. *Dev. Biol.* **261**, 289–312.

Saba R., Johnson J. E. and Saito T. (2005) Commissural neuron identity is specified by a homeodomain protein, Mbh1, that is directly downstream of Math1. *Development* **132**, 2147–2155.

Sanes J. R. and Lichtman J. W. (1999) Development of the vertebrate neuromuscular junction. *Annu. Rev. Neurosci.* **22**, 389–442.

Sgard F., Charpantier E., Bertrand S., Walker N., Caput D., Graham D., Bertrand D. and Besnard F. (2002) A novel human nicotinic receptor subunit, alpha10, that confers functionality to the alpha9-subunit. *Mol. Pharmacol.* **61**, 150–159.

Sheard P. W. and Duxson M. J. (1997) The transient existence of 'en passant' nerve terminals in normal embryonic rat skeletal muscle. *Brain Res. Dev. Brain Res.* **98**, 259–264.

Sine S. M. and Claudio T. (1991) Gamma- and delta-subunits regulate the affinity and the cooperativity of ligand binding to the acetylcholine receptor. *J. Biol. Chem.* **266**, 19369–19377.

Vernino S., Amador M., Luetje C. W., Patrick J. and Dani J. A. (1992) Calcium modulation and high calcium permeability of neuronal nicotinic acetylcholine receptors. *Neuron* **8**, 127–134.

Vetter D. E., Liberman M. C., Mann J., Barhanin J., Boulter J., Brown M. C., Saffiote-Kolman J., Heinemann S. F. and Elgoyhen A. B. (1999) Role of alpha9 nicotinic ACh receptor subunits in the development and function of cochlear efferent innervation. *Neuron* **23**, 93–103.

Wang Z. Z., Washabaugh C. H., Yao Y., Wang J. M., Zhang L., Ontell M. P., Watkins S. C., Rudnicki M. A. and Ontell M. (2003) Aberrant development of motor axons and neuromuscular synapses in MyoD-null mice. *J. Neurosci.* **23**, 5161–5169.

Weintraub H. (1993) The MyoD family and myogenesis: redundancy, networks, and thresholds. *Cell* **75**, 1241–1244.

Westerman B. A., Murre C. and Oudejans C. B. (2003) The cellular Pax-Hox-helix connection. *Biochim. Biophys. Acta* **1629**, 1–7.

Woods C., Montcouquiol M. and Kelley M. W. (2004) Math1 regulates development of the sensory epithelium in the mammalian cochlea. *Nat. Neurosci.* **7**, 1310–1318.

Yamane A., Saito T., Nakagawa Y., Ohnuki Y. and Saeki Y. (2002) Changes in mRNA expression of nicotinic acetylcholine receptor subunits during embryonic development of mouse masseter muscle. *Zoolog. Sci.* **19**, 207–213.

Yang Q., Bermingham N. A., Finegold M. J. and Zoghbi H. Y. (2001) Requirement of Math1 for secretory cell lineage commitment in the mouse intestine. *Science* **294**, 2155–2158.

Zhao P., Seo J., Wang Z., Wang Y., Shneiderman B. and Hoffman E. P. (2003) In vivo filtering of in vitro expression data reveals MyoD targets. *C R Biol.* **326**, 1049–1065.

Zheng J. L. and Gao W. Q. (2000) Overexpression of Math1 induces robust production of extra hair cells in postnatal rat inner ears. *Nat. Neurosci.* **3**, 580–586.

